K1DM3 Design Note

Finite Element Analysis of the Mirror Mounts for the K1DM3 Project

Version 1.4.1, January 30, 2014

By Jerry Cabak, Jerry Nelson, J. Xavier Prochaska

I. Overview

The tertiary mirror (M3) on the Keck I telescope (K1) feeds light into the Nasmyth and bent-Cassegrain foci of the telescope. The Keck I Deployable Tertiary Mirror (K1DM3) will replace the existing Keck I tertiary mirror with a new optical element designed to provide a field-of-view (FOV) of $5'$ at the Nasmyth foci.

This document details the preliminary design work completed to derive a design for the mirror support, especially the number and placement of axial supports. These were established by evaluating outputs on deflections of the mirror under gravity using a standard finite element analysis (FEA). We also analyzed deflections related to the lateral support to confirm its performance. Future work will establish the design of the wiffle tree structure.

II. Model Parameters

The program ANSYS was used to perform the FEA modeling. The following parameters related to the mirror and its supports were:

- Major diameter of mirror: 881.2 mm
- Minor diameter of mirror: 622.4 mm
- Center hole dia for lateral support: 150 mm
- Hole depth for lateral support: 36 mm
- Axial support pads: 15 mm dia
- Mirror thickness: 50 mm
- Mirror material: Zerodur
- Mirror weight: $\sim$53 kg

III. Finite Element Analysis of the Mirror Mounts

The modeling and static deflection analysis was performed with traditional 3D, 20-node brick elements which yield only displacements (3 degrees of freedom) at the nodal locations. To obtain slopes (rotations) and reasonable statistics the surface deformations of the top surface were mapped to a more dense and inform shell model. Results of this second model provided the surface slopes (and deflections) over a uniformly distributed surface. These results were exported to Excel for easy processing to obtain statistical values (max, min, rms, etc.)

A. Design Requirements

The mirror support system is intended to hold the mirror at its ideal shape, i.e. a flat surface, to acceptable tolerances. A full description of the mirror specifications regarding flatness and slopes is provided in the Design Note *Mirror Specs, v1.2.2.* These specify a maximum 57nm RMS surface error and 1.68×10^{-6} RMS slope error ($0.35''$). These requirements guide the following design.

B. Axial Supports

We may begin by estimating the gravity deflections of a N-point axial support system as a function of the size and thickness of the mirror. This can be done relatively easily using "analytic" expressions.

The minimum RMS gravity deflections of a mirror on an N-point support are given by

$$\sigma_N = \gamma_N (q/D)(A/N)^2 \tag{1}$$

where σ is the RMS surface error under full axial gravity loading, γ_N is the support point efficiency (Thirty Meter Telescope [TMT] report #74), q is the gravity load/area, D is the "bending", and A is the mirror area. Taking $N = 12$ and assuming the properties for Zerodur glass, we derive

$$\sigma_{12} = 4.09 \times 10^{-11} (\pi ab/h)^2 \quad . \tag{2}$$

For the dimensions of our elliptical mirror and taking $h = 0.050$m, we get $\sigma_{12} = 3.03 \times 10^{-9}$m.

This 12-point support system was the concept described in our MRI proposal to the NSF. It is evident from the analysis above, however, that this easily meets the design requirements on surface flatness. Therefore, we quickly moved to a 6-point support system in preliminary design as this greatly simplifies the design and should still easily satisfy the specifications.

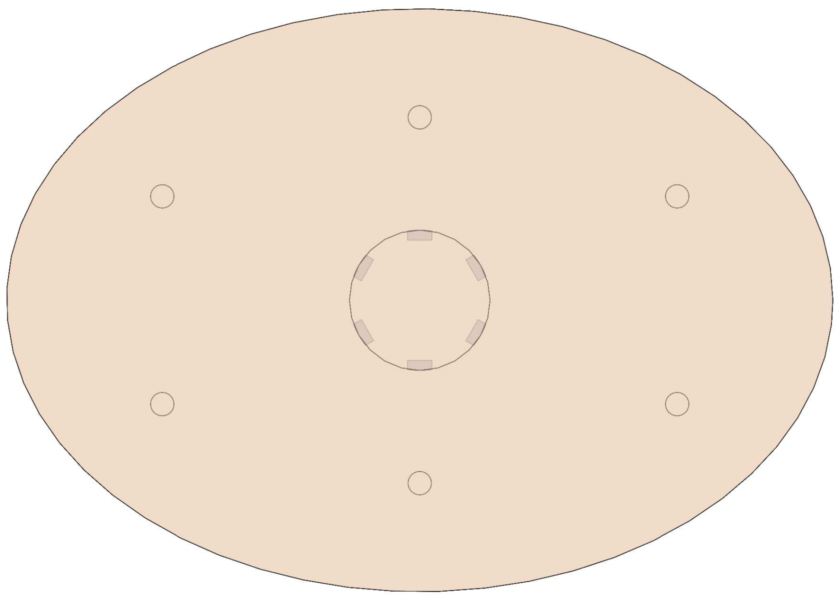

Fig. 1.— Sketch of the basic design for the mirror support, showing the orientation of the 6 axial pads and the locations of the radial pads for the lateral support at the center.

Figure 1 shows the basic design and the chosen orientation of the axial pads and the inner radial pads for the lateral support. The FEA started with finding the optimal location for the axial pads. Worst case deformation of the mirror would occur with gravity normal to the surface. For this analysis a 1/4 symmetry model was used. Figure 2 shows the model geometry. The finite element mesh consisted of 32,121 nodes and 12,768 elements. The placement of the support pads (two small circles in Figure 2) was controlled with three variables. For the pad on the minor axis, only the distance (Y1) from the center was varied. The other pad was located with both X and Y coordinates (X2, Y2).

The model was small and the analysis ran in less than a minute. It was relatively easy to iterate, setting new values for the locations and rerunning until best coordinates were obtained for the least amount of deformation; the primary goal was to minimize the peak-to-valley value over the entire surface.

The resulting best coordinates were:

- X1 = .19525 m
- X2 = .275 m
- Y2 = .111 m

The two supports on the minor diameter are therefore spaced .3905 m apart. The remaining four supports form a rectangle with dimensions .55 m × .222 m, as shown in Figure 1.

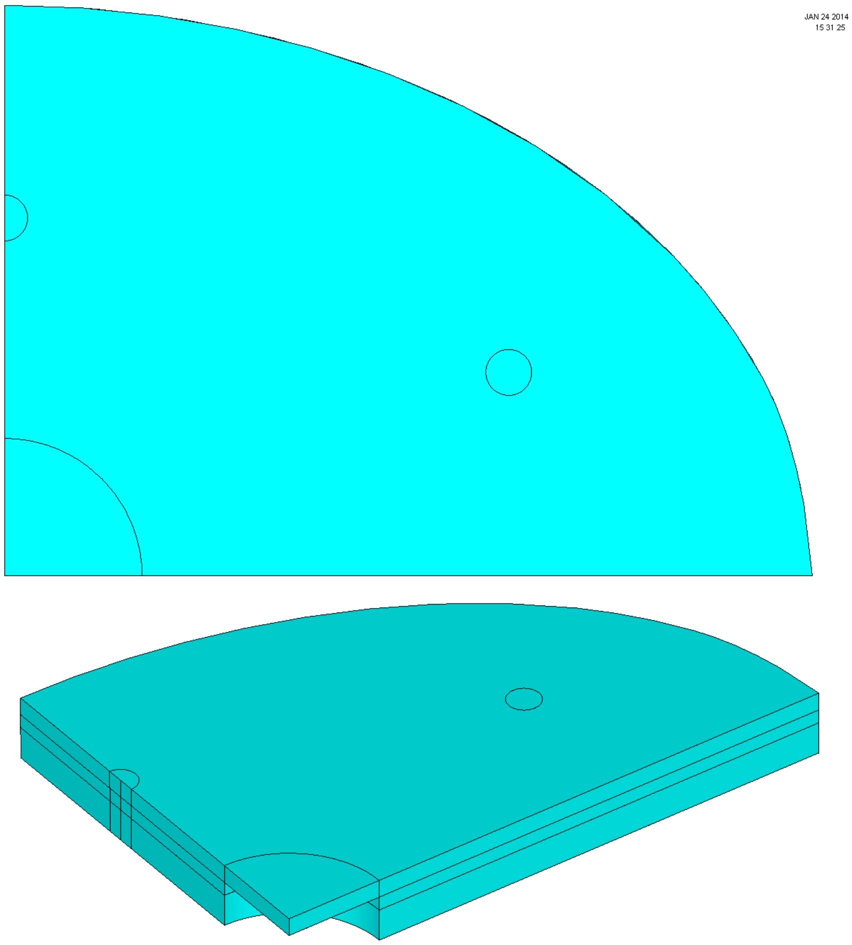

Fig. 2.— Top and isometric views of the FEA solid geometry showing the axial pad locations and the center hole for the lateral support.

Deflections normal to the mirror surface are shown in Figure 3. Figure 3a shows deflections for the entire model while Figure 3b is a plot of deflections for the surface only. A summary of the deflections and slopes is shown in Table 1.

Table 1: Surface Deflections and Slopes for the 1/4 Symmetry Model

Parameter	Deflection (nm)	Slope[a] (arc-sec)
Maximum	−18.7	.121
Minimum	−107.5	−.116
Peak-to-valley	88.8	.237
RMS	20.4	.062

[a]Slope extremes from both directions.

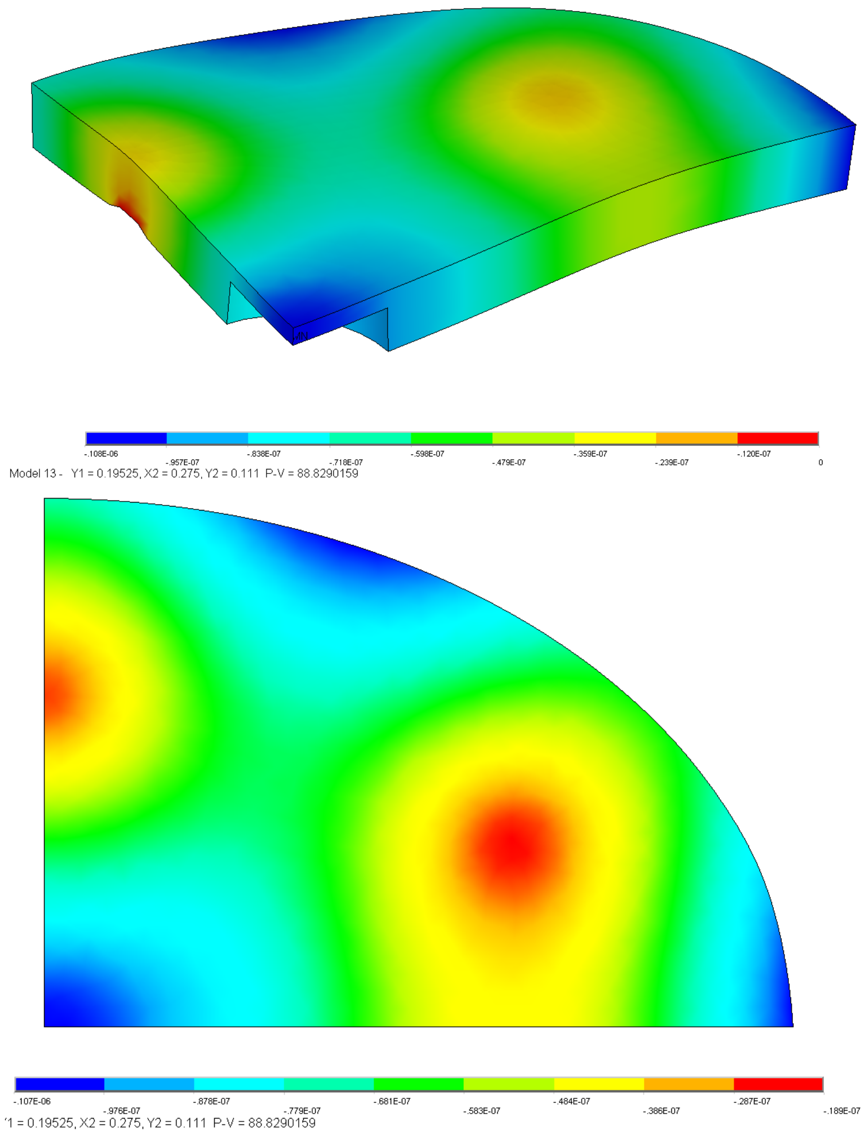

Fig. 3.— Displacement contour plots. The displacement plotted is deflection in the direction of the surface normal. The top image shows the displacements plotted over the exaggerated deformation of the mirror. The legend bar is scaled over the entire model. The lower image is the same displacement but only for the top surface of the mirror. The legend bar is scaled only over the top surface.

C. Lateral Support

To study the effectiveness and performance of the lateral support, design gravity loads were now applied in the plane of the mirror. Two additional 1/2 symmetry models were created to consider gravity in each of the two orthogonal directions; along the major and minor axes. The model for gravity along the minor axis is shown in Figure 4. Figure 5 shows the model for gravity in the other direction, i.e. along the major axis. Table 2 shows the deformation and slope results for these cases. The three gravity cases analyzed (normal to surface & two orthogonal directions in the plane of the mirror) represent the extreme conditions that can be imposed on the mirror. As the telescope moves during operation, the mirror deformations will vary between these limits in combinations proportional to the gravity vector.

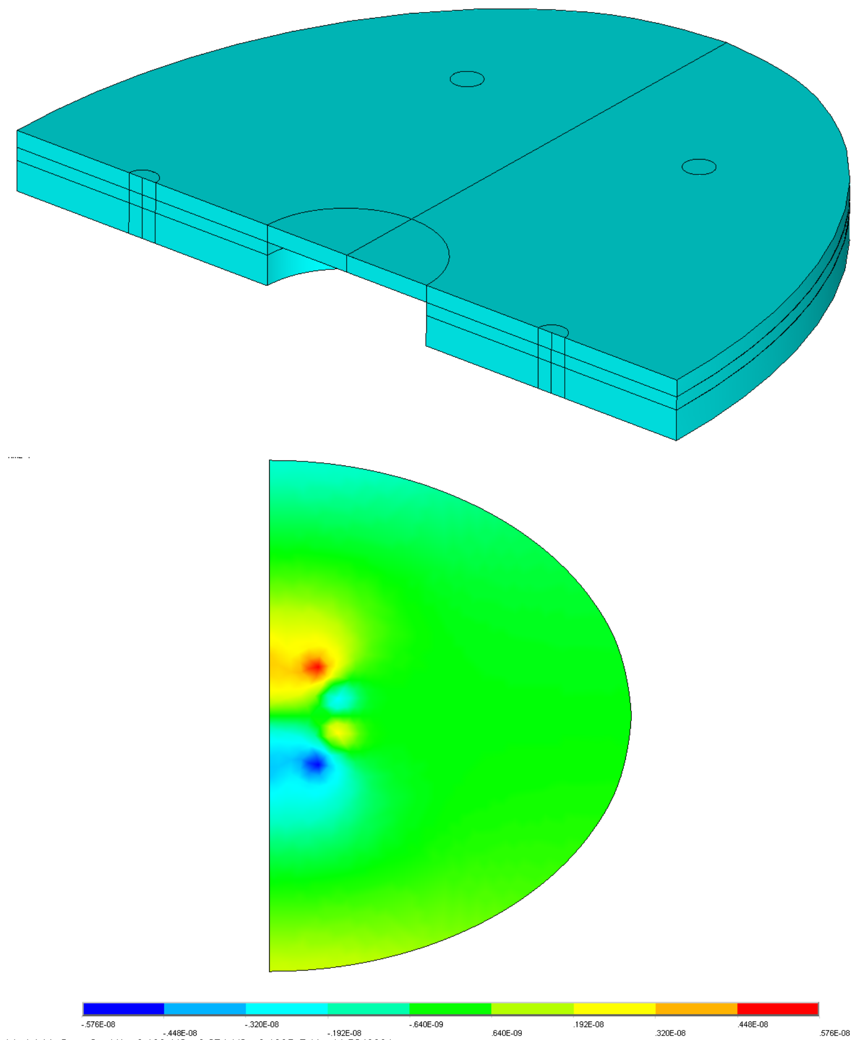

Fig. 4.— FEA model for lateral support with gravity along the minor axis. (top) Isometric view of the FEA solid geometry showing the axial pad locations and the center hole for the lateral support. (bottom) Displacement for the top surface of the mirror.

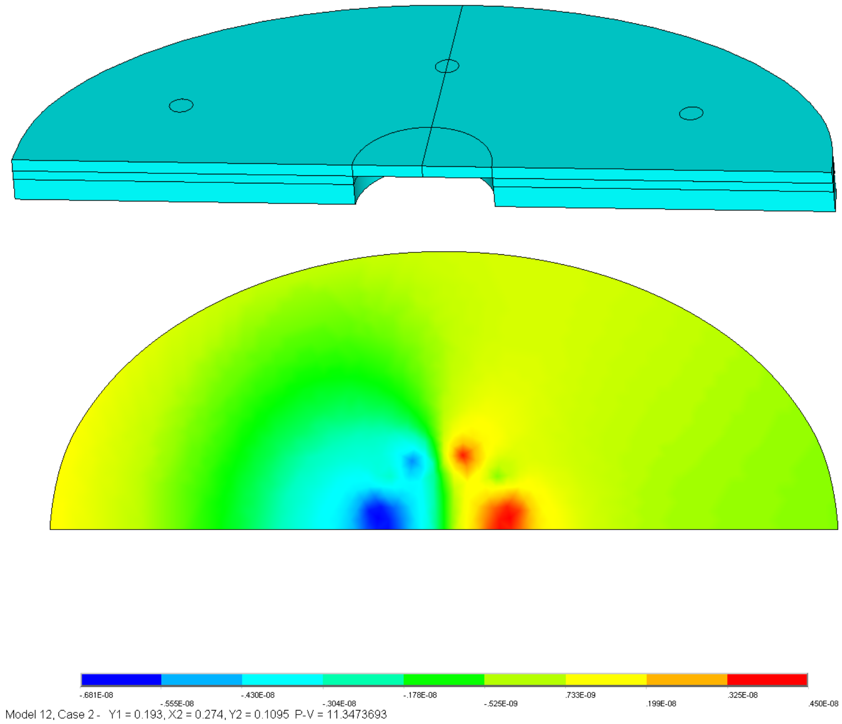

Fig. 5.— Same as Figure 4 but for for gravity along the major axis.

Table 2: Surface Deflections and Slopes for Lateral Support Models

	Minor Axis Gravity		Major Axis Gravity	
Parameter	Deflection (nm)	Slope[a] (arc-sec)	Deflection (nm)	Slope[a] (arc-sec)
Peak-to-valley	11.2	0.086	11.3	0.075
RMS	1.1	0.006	1.4	0.003

[a]Slope extremes from both directions.

C. Other Design Considerations

The pervious sections described the design and performance of our preliminary design for the mirror mounts. We also considered an alternative axial pad arrangement where two supports are on the major axis. This arrangement also gave good results, $\sim 85-90$nm P-V. Jerry Nelson recommends the layout shown in Figure 1 (supports on the minor axis) because the mirror will be moving between deployed and stowed positions along the major axis. Furthermore, a wiffle tree support system for this configuration will have symmetry in the plane of motion.

Another possible orientation of the axial pads is to clock them by 30 deg. Results for this case give very similar deflections and slopes. The orientation shown in Figure 1, however, maps more directly with the axial pads; and the results for the two lateral gravity cases were closer to each other in results. This drives the orientation of the chosen design.